

## Research paper

# Nkx6.1 enhances neural stem cell activation and attenuates glial scar formation and neuroinflammation in the adult injured spinal cord

Misaal Patel<sup>a</sup>, Jeremy Anderson<sup>a</sup>, Shunyao Lei<sup>a</sup>, Zachary Finkel<sup>a</sup>, Brianna Rodriguez<sup>a</sup>, Fatima Esteban<sup>a</sup>, Rebecca Risman<sup>a</sup>, Ying Li<sup>a,1</sup>, Ki-Bum Lee<sup>a,b</sup>, Yi Lisa Lyu<sup>c,2</sup>, Li Cai<sup>a,\*</sup>

<sup>a</sup> Department of Biomedical Engineering, Rutgers University, 599 Taylor Road, Piscataway, NJ 08854, USA

<sup>b</sup> Department of Chemistry and Chemical Biology, Rutgers University, 123 Bevier Road, Piscataway, NJ 08854, USA

<sup>c</sup> Department of Pharmacology, Rutgers University-Robert Wood Johnson Medical School, 675 Hoes Lane, Piscataway, NJ 08854, USA

## ARTICLE INFO

## Keywords:

Nkx6.1  
Spinal cord injury  
Neural stem progenitor cell  
Lentivirus  
Gene expression  
Astrogliosis  
Glial scar  
Neuroinflammation

## ABSTRACT

Nkx6.1 plays an essential role during the embryonic development of the spinal cord. However, its role in the adult and injured spinal cord is not well understood. Here we show that lentivirus-mediated Nkx6.1 expression in the adult injured mouse spinal cord promotes cell proliferation and activation of endogenous neural stem/progenitor cells (NSPCs) at the acute phase of injury. In the chronic phase, Nkx6.1 increases the number of interneurons, reduces the number of reactive astrocytes, minimizes glial scar formation, and represses neuroinflammation. Transcriptomic analysis reveals that Nkx6.1 upregulates the sequential expression of genes involved in cell proliferation, neural differentiation, and Notch signaling pathway, downregulates genes and pathways involved in neuroinflammation, reactive astrocyte activation, and glial scar formation. Together, our findings support the potential role of Nkx6.1 in neural regeneration in the adult injured spinal cord.

## 1. Introduction

In the adult mammalian spinal cord, there are several different cell populations that possess properties of neural stem cell or progenitor cell, e.g., ependymal cells, oligodendrocyte progenitors, and NG2+ cells (Kirdajova and Anderova, 2020; Sabelstrom et al., 2014). These neural stem progenitor cells (NSPCs) persist in the mammalian central nervous system and represent a promising cell source for damage repair and regeneration after spinal cord injury (SCI). However, the majority of injury-activated NSPCs differentiate into astrocytes and oligodendrocytes (Meletis et al., 2008; Mothe and Tator, 2005; Sabelstrom et al., 2014). In addition, injury-induced reactive astrocytes secrete chondroitin sulfate proteoglycans (CSPGs), which constitute most glial scars post-SCI (Milich et al., 2019; Soderblom et al., 2013). Despite extensive research, promoting neuronal regeneration and reducing the glial scar after SCI have been extremely difficult. Studies have shown that resident non-neuronal cells can be converted to mature neurons by forced expression of certain transcription factors, e.g., NeuroD1 and Sox2

(Chen et al., 2017; Su et al., 2014). Due to low reprogramming efficiency, the converted neurons show limited to no benefit in functional recovery (Su et al., 2014).

NG2 cells are known to be oligodendrocyte progenitor cells and located throughout the central nervous system, and they serve as a pool of progenitors to differentiate into oligodendrocytes (Kirdajova and Anderova, 2020; Nishiyama et al., 2009). In response to SCI, NG2 cells increase their proliferation and differentiation into remyelinating oligodendrocytes (Hackett et al., 2016; Hackett and Lee, 2016). SCI induces transient doublecortin (DCX) expression in NG2 glia but not astrocytes or ependymal cells. In addition, SOX2 promotes NG2 glia to generate propriospinal neurons and contributes to behavioral improvements (Tai et al., 2021).

Our previous studies have established that NK6 Homeobox 1 (Nkx6.1) regulates Notch signaling in NSPCs (Li et al., 2016; Tzatzalos et al., 2012). Nkx6.1 is widely expressed by NSPCs within the neural tube (Cai et al., 2000). Nkx6.1 plays a critical role in ventral neural patterning and controls the lineage specification of both neurons and

\* Corresponding author at: Department of Biomedical Engineering, Rutgers University, 599 Taylor Road, Piscataway, NJ 08854, USA.

E-mail address: [lcai@rutgers.edu](mailto:lcai@rutgers.edu) (L. Cai).

<sup>1</sup> Current affiliation: Department of Physiology and Pathophysiology, Xi'an Jiaotong University School of Basic Medical Sciences, Shaanxi Engineering and Research Center of Vaccine, Key Laboratory of Environment and Genes Related to Diseases of Education Ministry of China, Xi'an, Shaanxi 710000, China.

<sup>2</sup> Current affiliation: Innovation Ventures, Rutgers University, 33 Knightsbridge Road, Piscataway, NJ 08854, USA.

glia during spinal cord development (Sander et al., 2000; Zhao et al., 2014). In the adult mouse spinal cord, Nkx6.1<sup>+</sup> cells retain the proliferative property of NSPCs (Fu et al., 2003). In the injured spinal cord of zebrafish, V2 interneurons can be generated from Pax6 and Nkx6.1 expressing progenitors (Kuscha et al., 2012). Nkx6.1 is also known to promote differentiation of NSPCs into mature neurons during the development of the spinal cord (Briscoe et al., 1999) and after injury in turtles (Fabbiani et al., 2018).

In this study, we aim to determine the role of Nkx6.1 in regulating cell proliferation, NSPC activation and neurogenesis in the adult injured spinal cord. Lentivirus gene delivery system was used to express Nkx6.1 in the adult mouse with a lateral hemisection SCI. We show that Nkx6.1 expression increases NSPC activation and proliferation in the acute phase of SCI. In the chronic phase of SCI, Nkx6.1 expression increases the number of cholinergic interneurons and reduces neuroinflammation and glial scar formation. Transcriptomic analysis reveals that Nkx6.1 expression correlates with 1) upregulation of genes and signaling pathways (i.e., Notch signaling and Wnt signaling) involved in NSPC activation and axon guidance, and 2) downregulation of genes and signaling pathways associated with neuroinflammation and reactive astrocytes. These findings unveil the role of Nkx6.1 in promoting neurogenesis and inhibiting reactive astrocytes and glial scar formation in the adult spinal cord after injury. Thus, the expression of Nkx6.1 in the adult injured spinal cord represents a potential approach to manipulate NSPCs for damage repair and neuronal regeneration.

**2. Results**

Given the established role of Nkx6.1 in neurogenesis (Sander et al., 2000), in astrocyte progenitor specification (Zhao et al., 2014), and in Notch signaling regulation (Li et al., 2016) during the embryonic development of the spinal cord, we postulate that forced Nkx6.1 expression in the adult spinal cord promotes neural regeneration after SCI. To test this hypothesis, we performed lateral hemisection SCI at

thoracic (T) 10 level in 8–12 weeks old mice. Immediately after SCI, lentivirus encoding Nkx6.1 and a red fluorescent protein (RFP) reporter (lenti-Nkx6.1-RFP) was delivered ~1 mm rostral and caudal to the injury site (Fig. 1A and Fig. S1A). A lentivirus encoding only the reporter RFP (lenti-Ctrl-RFP) was used as a control. The success and reproducibility of the lateral hemisection injury were determined by paralysis in the left hind limb at 0 day-post injury (0 DPI) and 1 DPI. Next, we performed cellular and molecular analysis on spinal cord samples using immunohistochemistry (IHC), RNA-sequencing (RNA-seq), real-time quantitative reverse transcription polymerase chain reaction analysis (qRT-PCR or qPCR), and locomotor functional assessment with open field test (BMS score) at various days post-injury (DPI; Fig. 1B). For each experimental and control group, e.g., sham (only exposing the spinal cord without injury), injured spinal cord with lenti-Ctrl-RFP injection (SCI + Ctrl), and injured spinal cord with lenti-Nkx6.1-RFP injection (SCI + Nkx6.1; n ≥ 3 for each group and time-point). Lentivirus-mediated Nkx6.1 expression in the spinal cord tissues at 3 DPI was confirmed by qPCR analysis (Fig. S1B). Next, we examined the composition of virally transduced cells using cell-specific markers, e.g., NeuN for neurons, GFAP for astrocytes, and NG2 for oligodendrocytes. Immunofluorescence staining was performed on sagittal sections of the spinal cord tissues. No significant difference was detected between the SCI + Ctrl group and SCI + Nkx6.1 group, indicating the lentivirus does not preferentially target a specific cell type (Fig. S2).

**2.1. Nkx6.1 enhances cell proliferation during the acute phase of SCI**

Studies have established the role of Nkx6.1 in regulating cell proliferation in rat pancreatic islets (Tessem et al., 2014) and in the lesion-induced generation of interneurons in the adult zebrafish spinal cord (Kuscha et al., 2012). Thus, we examined the effect of Nkx6.1 on cell proliferation via IHC using an antibody against Ki67 at 3 DPI (Fig. 2A). We detected ~1% of Ki67<sup>+</sup> cells among DAPI<sup>+</sup> cells in the sham group. In contrast, SCI significantly increased the percentage of Ki67<sup>+</sup> cells

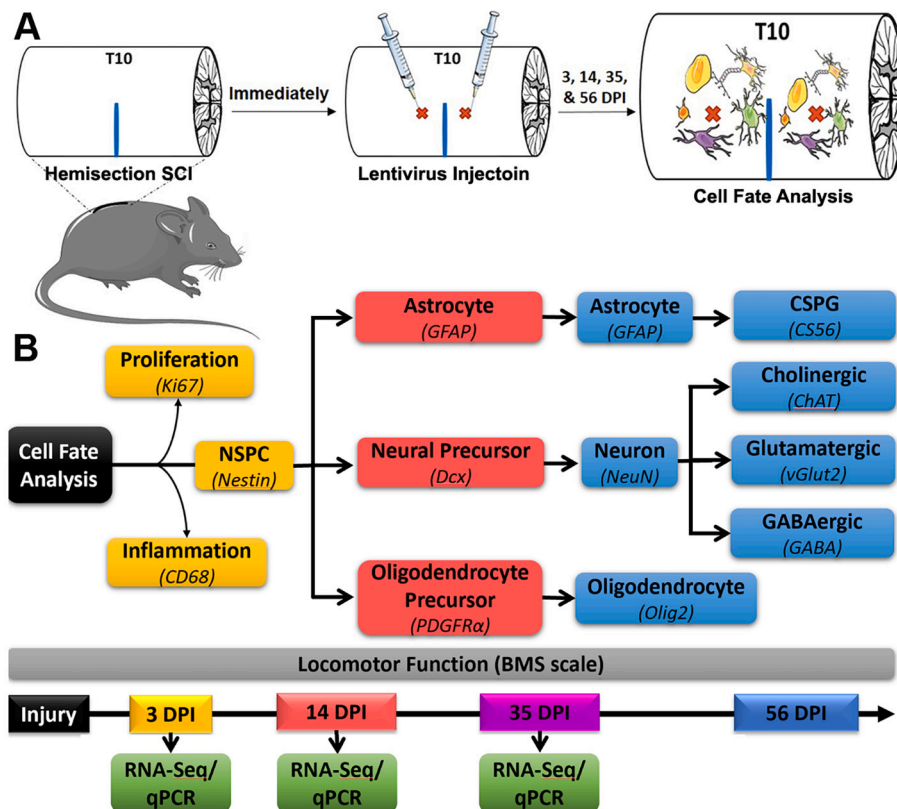


**Fig. 1.** Experimental scheme. (A) Lateral hemisection SCI was performed on 8–12 weeks old mice at the thoracic vertebrae (T10) level followed by injection of lenti-Nkx6.1-RFP virus. Lentivirus encoding only the reporter RFP (lenti-Ctrl-RFP) serves as a control for viral infection. Animals received surgery only to expose the spine were sham group. Spinal cord segments (~5–6 mm) at the injection site were harvested at 3, 14, 35, and 56 DPI to determine effect of Nkx6.1 on cellular and molecular changes using immunohistochemistry (IHC), RNA-Seq, Ingenuity Pathway Analysis (IPA), and quantitative Real-time PCR analysis (qPCR). (B) Schematic depiction of cell fate analysis following SCI and lentiviral injection. n = 3/group/timepoint. DPI = days post injury.

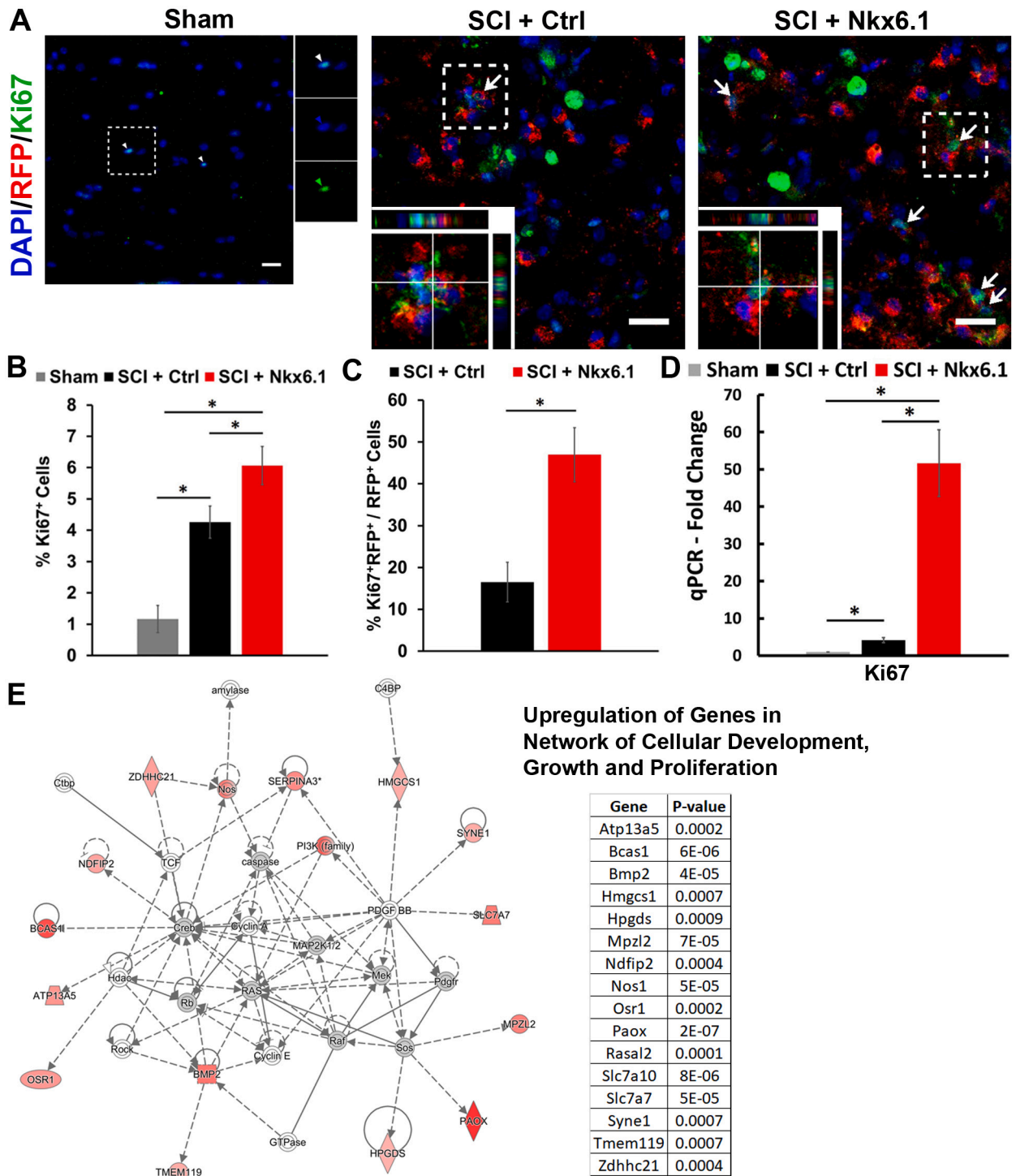


**Fig. 2.** Nkx6.1 increases cell proliferation in the injured spinal cord.

Spinal cord tissues were harvested 3 DPI and analyzed for the effect of Nkx6.1 expression on cell proliferation. (A) Representative confocal images of the sagittal section around the injection site. Bottom left shows a higher magnification of an orthogonal view of the area denoted by a white box. Arrows indicate the co-labeling of the virally transduced cells with Ki67. Nuclei were counterstained with DAPI. Scale bars = 20  $\mu$ m. Quantification of the percentage of Ki67<sup>+</sup> cells among DAPI<sup>+</sup> cells (B) and among RFP<sup>+</sup> cells (C). (D) qPCR analysis of the mRNA level of Ki67, as normalized to the sham group. (E) Nkx6.1-induced upregulation (indicated by pink) of genes in network of cellular development, growth and cell proliferation revealed by RNA-Seq and IPA analysis. n = 3/group for IHC, RNA-Seq, and qPCR, respectively. Mean  $\pm$  SEM; One-way ANOVA followed by Tukey post-hoc test or Student's *t*-test. \**p*-value < 0.05 is considered as statistically significant. (For interpretation of the references to colour in this figure legend, the reader is referred to the web version of this article.)

among the DAPI<sup>+</sup> cells around the injury and injection site in both the SCI + Ctrl group and SCI + Nkx6.1 group. However, Nkx6.1 expression further increased the percentage of Ki67<sup>+</sup> cells among DAPI<sup>+</sup> cells (Fig. 2B). When compared with the virally transduced cells (RFP<sup>+</sup>),

there was a significantly higher percentage of Ki67<sup>+</sup>/RFP<sup>+</sup> co-labeled cells among RFP<sup>+</sup> cells in the SCI + Nkx6.1 group (Fig. 2C and Fig. S3). The upregulation in cell proliferation was validated by measuring the mRNA level of Ki67 via qPCR analysis (Fig. 2D). To

identify the molecular networks affected by Nkx6.1 expression in the injured spinal cord, we performed RNA-seq analysis and identified 3425 and 1973 genes that were significantly differentially expressed ( $p < 0.05$ ) between the SCI + Ctrl ( $n = 3$ ) and SCI + Nkx6.1 ( $n = 3$ ) groups at 3 and 35 DPI, respectively (Fig. S4). Ingenuity Pathway Analysis (IPA) and gene ontology analysis of the differentially expressed genes (DEGs) reveal that Nkx6.1-induced genes, signaling pathways and networks were involved in the networks for cellular development, axonal guidance, and cell proliferation (Fig. 2E and Fig. S5). These results support the role of Nkx6.1 in promoting cell proliferation in the injured spinal cord.

2.2. Nkx6.1 increases NSPC activation at the acute phase of SCI

To investigate the effect of Nkx6.1 expression on the level of NSPC activation after SCI, we conducted IHC analysis using a NSPC marker Nestin on sagittal sections of the spinal cord tissues at 3 DPI (Fig. 3A). An increased number of Nestin<sup>+</sup> cells was observed around the injury and injection sites compared to the sham animals (Fig. S6). Nkx6.1 expression ( $n = 3$ ) significantly increased the percentage of Nestin<sup>+</sup>/RFP<sup>+</sup> cells

among RFP<sup>+</sup> cells as compared to the SCI + Ctrl group ( $n = 3$ ; Fig. 3A-C). The increase in the number of Nestin<sup>+</sup> cells was validated by the mRNA level of Nestin through the qPCR analysis (Fig. 3D).

2.3. Nkx6.1 expression transiently promotes Notch signaling during the acute phase of SCI

The Notch signaling pathway plays an essential role in the maintenance and differentiation of adult NSPCs (Yamamoto et al., 2001). Thus, we examined the effect of Nkx6.1 on the expression of Notch1 and genes involved in the Notch signaling pathway. We observed a significant increase in the number of Notch1<sup>+</sup>/RFP<sup>+</sup> co-labeled cells among RFP<sup>+</sup> cells in the SCI + Nkx6.1 group as compared to the SCI + Ctrl group at 3 DPI by IHC analysis (Fig. 4A). The RNA-seq followed by IPA analysis further revealed that Nkx6.1 expression ( $n = 3$ ) upregulated genes involved in the Notch signaling pathways at 3 DPI but not at 35 DPI (Fig. 4B-C). The qPCR analysis confirmed that Nkx6.1 expression increased the mRNA level of Notch1 (Fig. 4D), Jag1 and Jag2 at 3 DPI (Fig. 4E). Thus, Nkx6.1-induced NSPC activation correlates with an upregulation of Notch signaling pathway during the acute phase of SCI.

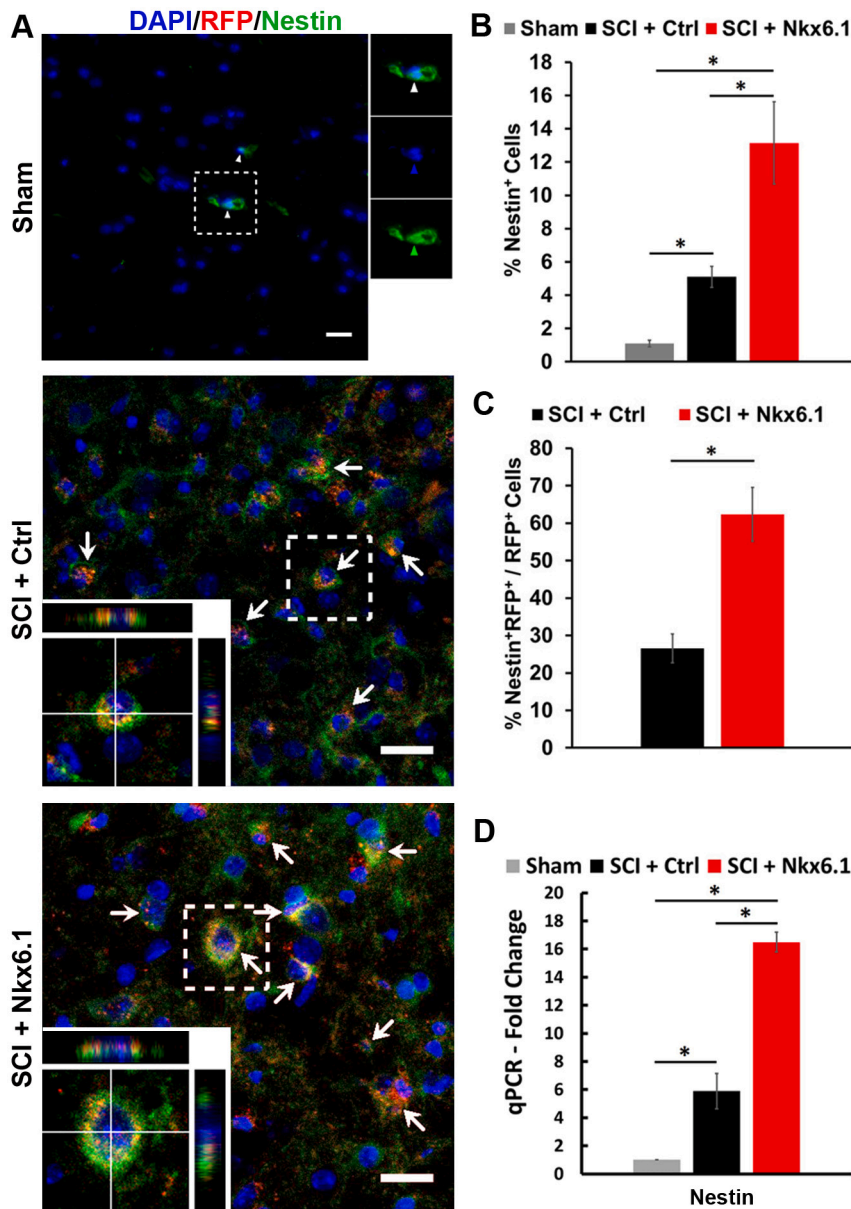
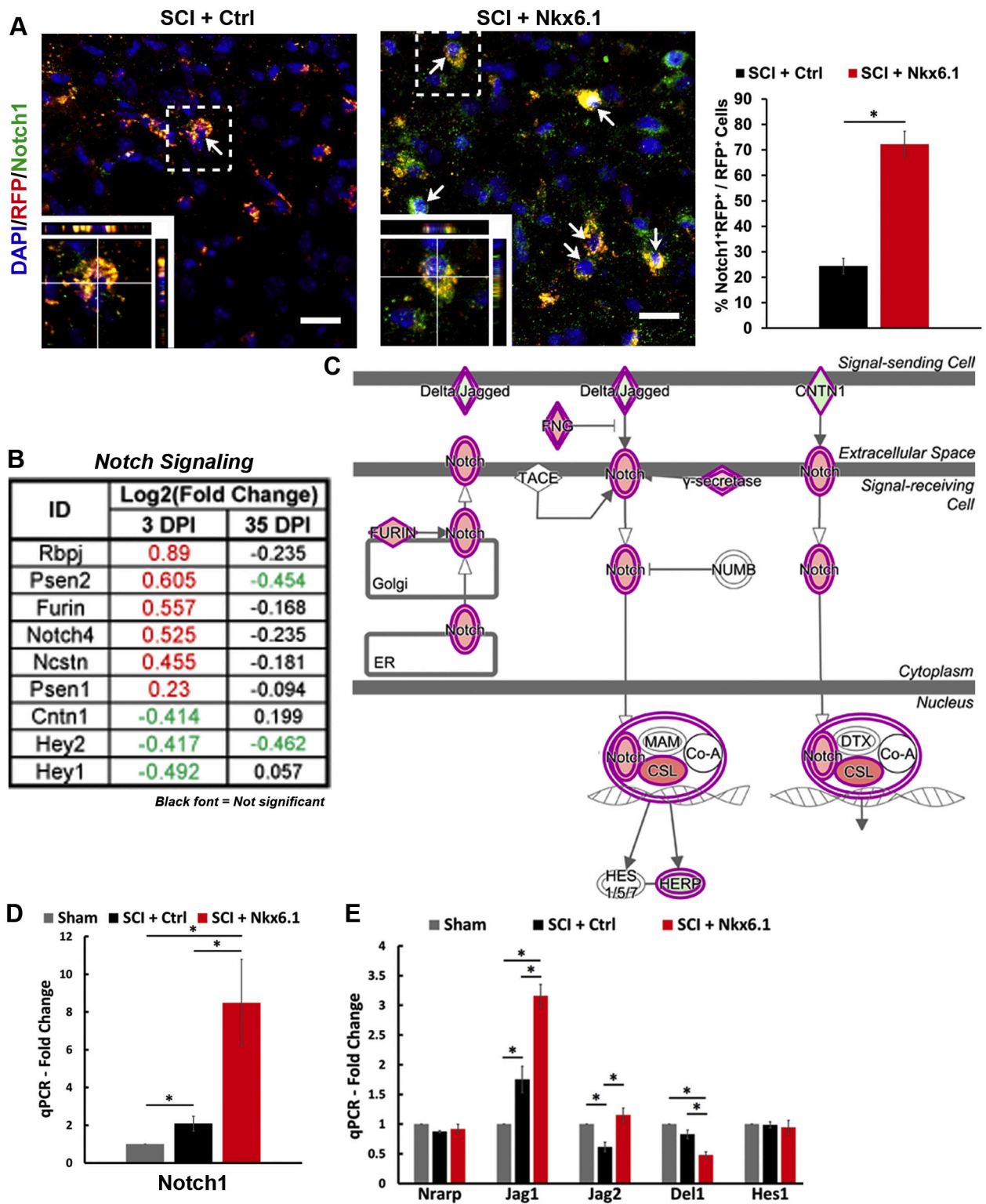


Fig. 3. Nkx6.1 increases NSPC activation in the injured spinal cord. Spinal cord tissues were harvested at 3 DPI and analyzed for the effect of Nkx6.1 expression on NSPC activation. (A) Representative confocal images of the sagittal section around the injection site. The bottom left shows a higher magnification of an orthogonal view of the area denoted by a white box. Arrows indicate the co-labeling of the virally transduced cells with Nestin. Scale bars = 20  $\mu$ m. Quantification of the percentage of Nestin<sup>+</sup> cells among DAPI<sup>+</sup> cells (B) and Nestin<sup>+</sup>/RFP<sup>+</sup> cells among RFP<sup>+</sup> cells (C). (D) qPCR analysis of the mRNA level of Nestin, normalized to the sham group.  $n = 3$ /group for IHC, RNA-Seq, and qPCR. Mean  $\pm$  SEM; One-way ANOVA followed by Tukey post-hoc test or Student's t-test. \*  $p$ -value  $< 0.05$ .



**Fig. 4.** Nkx6.1 transiently upregulates Notch signaling pathway at the acute phase of SCI. Spinal cord tissues were harvested at 3 DPI and analyzed for Nkx6.1 expression induced Notch signaling. (A) Representative confocal images and quantification of the percentage of Notch1<sup>+</sup> cells among RFP<sup>+</sup> cells at 3 DPI. Bottom left shows a higher magnification of an orthogonal view of the area denoted by a white box. Arrows indicate the co-labeling of the virally transduced (RFP<sup>+</sup>) cells with Notch1<sup>+</sup> cell. Nuclei were counterstained with DAPI. Scale bars = 20 μm; n = 3. Mean ± SEM; One-way ANOVA followed by Tukey post-hoc test and Student's *t*-test. \* *p*-value < 0.05. (B) A list of differentially expressed genes (DEGs) associated with Notch signaling pathway along with their log2(fold change) at 3 DPI and 35 DPI identified by RNA-seq analysis. (C) The ingenuity pathway analysis (IPA) of the DEGs revealed that Nkx6.1 expression transiently activates Notch signaling pathway. (D-E) qPCR analysis of genes (Notch1, Nrarp, Jag1, Jag2, Del1, and Hes1) involved in the Notch signaling pathway, normalized to the sham level at 3 DPI.

## 2.4. *Nkx6.1 increases the number of cholinergic interneurons in the adult injured spinal cord*

To determine the effect of *Nkx6.1* on neural regeneration in the injured spinal cord, we examined the identity of RFP<sup>+</sup> cells at 14 DPI with markers for neuronal progenitors/neuroblasts (doublecortin or DCX), astrocytes (GFAP), and oligodendrocyte progenitors (PDGFR $\alpha$ ; Fig. 5A). Some of the DCX<sup>+</sup>/RFP<sup>+</sup> cells show small multipolar processes, a typical immature neuronal morphology. Compared to the SCI + Ctrl group, *Nkx6.1* expression significantly increased the number of DCX<sup>+</sup>/RFP<sup>+</sup> cells and decreased the number of PDGFR $\alpha$ <sup>+</sup>/RFP<sup>+</sup> cells among RFP<sup>+</sup> cells and no significant differences in GFAP<sup>+</sup>/RFP<sup>+</sup> cells (Fig. 5C). We further determined the cellular composition and gene expression changes at 56 DPI using a mature neuronal marker NeuN, a cholinergic neuronal marker ChAT, a glutamatergic neuronal marker vGlut2, and a GABAergic neuronal marker GABA (Fig. 5B). We found a significant increase in the number of NeuN<sup>+</sup> and ChAT<sup>+</sup> cells, with no significant difference in GABA<sup>+</sup> or vGlut2<sup>+</sup> cells in the SCI + *Nkx6.1* group as compared to the SCI + Ctrl group (Fig. 5D). In addition, no significant differences were detected in the number of Olig2<sup>+</sup> cells among virally transduced RFP<sup>+</sup> cells (Fig. S7). The qPCR analysis confirmed that *Nkx6.1* expression increased the mRNA level of NeuN (Hrnp3) and ChAT and decreased Tph1 (Tryptophan hydroxylase 1, a serotonergic neuronal marker) mRNA level compared to the SCI + Ctrl group at 35 DPI (n = 3 for all three groups, Fig. 5E). Furthermore, RNA-seq and IPA analysis on the spinal cord tissue samples at 35 DPI identified the upregulation of the genes known to promote synaptogenesis (Fig. S8A) and the downregulation of the genes known to inhibit synaptogenesis (Fig. S8B). The upregulation of some key genes involved in synapse formation and axon guidance (e.g., Syn1, Cttna1, Ntng1, and Col6a2) was confirmed by qPCR analysis (Fig. S8C).

## 2.5. *Nkx6.1 represses neuroinflammation in the adult injured spinal cord*

Neuroinflammation is a response from the innate immune system and plays an essential role in neural regeneration and functional recovery after SCI (Alexander and Popovich, 2009; Gensel and Zhang, 2015; Siddiqui et al., 2015). A widely accepted marker CD68 for neuroinflammation is present in activated microglia and macrophages after injury (McKay et al., 2007). To explore the potential effect of *Nkx6.1* expression on neuroinflammation, we stained the spinal cord sections with an antibody against CD68. We found a significantly reduced number of CD68<sup>+</sup> cells at the injury/injection sites in the SCI + *Nkx6.1* group compared to the SCI + Ctrl group (Fig. 6A-C). RNA-seq data analysis revealed that the signaling pathways associated with neuroinflammation, e.g., NF- $\kappa$ B signaling and Interleukin signaling, were significantly downregulated at both 3 DPI and 35 DPI by *Nkx6.1* expression (Fig. 6D). IPA analysis identified the top affected signaling pathway was the neuroinflammation pathway at 3 DPI (Fig. S9).

## 2.6. *Nkx6.1 attenuates reactive astrocytes and glial scar formation in the injured spinal cord*

SCI activates native astrocytes to become reactive astrocytes (RA), which secrete chondroitin sulfate proteoglycan (CSPG) into the extracellular space (McKeon et al., 1999). RA and CSPG contribute to the formation of glial scar (Jones et al., 2003; McKeon et al., 1995; Rhodes and Fawcett, 2004; Windle and Chambers, 1950). The glial scar inhibits transpassing axons; thus hinders the axon connections (Barnabe-Heider and Frisen, 2008; Fawcett and Asher, 1999; O'Shea et al., 2017). Thus, we examined the effect of *Nkx6.1* expression on astrogliosis and glial scar formation by immunostaining with a RA marker GFAP (Fig. 7A) and a CSPG marker CS56 (Fig. 7B) at 56 DPI. The level of GFAP and CS56 expression in the sham group established the baseline level of these proteins. Compared to the sham, injury increased the level of GFAP and CS56 protein expression in both the SCI + Ctrl group and SCI + *Nkx6.1*

group, while *Nkx6.1* expression significantly decreased the percentage of area immunostained with GFAP and CS56 at 56 DPI (Fig. 7C-D). This result indicates that *Nkx6.1* expression reduces astrogliosis and glial scar formation. Furthermore, our RNA-seq analysis showed *Nkx6.1* expression downregulated the known genes for RA (e.g., Ctnnb1 and Mmp13; Hara et al., 2017) and glial scar formation (e.g., Il1b, Bmp4, Bmp6, Tgfb1; Wang et al., 2018) as compared to the SCI + Ctrl group (n = 3 for all groups; Fig. 7E). These results indicate that *Nkx6.1* inhibits RA and glial scar formation in the injured spinal cord.

Lastly, we evaluated the effect of *Nkx6.1* expression on locomotor behavior from the day before the injury to 56 DPI using an open-field locomotion test. For each animal, a BMS score (Basso et al., 2006) was assigned double-blindly by three observers. The hemisection injury was performed on the left side of the spinal cord at T9–10 level and the right side of the spinal cord was intact (Fig. 8A), this affected the locomotor function only in the left hindlimb, and the locomotor function of the right hindlimb remains normal. We thus focused on the analysis of BMS scores from the left hindlimb. Although *Nkx6.1* expression promoted NSPC activation, increased the number of cholinergic neurons, and reduced inflammation and glial scar formation, a significant improvement in locomotor function was not observed (Fig. 8B).

## 3. Discussion

The lack of neurogenesis and formation of the glial scar are two major barriers that hinder tissue regeneration after SCI (O'Shea et al., 2017; Tran et al., 2018). In this study, we demonstrate that lentivirus-mediated *Nkx6.1* expression promotes cell proliferation and activation of endogenous NSPCs, which correlates with a transient upregulation of the Notch signaling in the acute phase of injury. *Nkx6.1* expression attenuates neuroinflammation and glial scar formation, which correlates with changes of gene expression involved in microglia and reactive astrocytes.

The hemisection injury is an ideal model for our study. It provides a direct comparison between injured and healthy tissue in the same animal; it is also suitable for examining locomotor function in different spinal tracts or comparing deficits in the function of contra- and ipsilateral lesions. In addition, hemisection results in a less severe injury than contusion or complete transection injury, and thus providing an easier/simpler postoperative animal care. However, it is more challenging to create a consistent injury with a partial transection model, and it can be difficult to determine whether the targeted tract is completely severed.

The Notch signaling pathway plays an essential role in stem cell self-renewal (Ables et al., 2011; Pierfelice et al., 2011). It is also actively involved in post-injury neural regeneration by regulating spontaneous cell proliferation, neurogenesis, synapse formation, and axon remyelination (Benner et al., 2013; Givogri et al., 2006; LeComte et al., 2015).

Studies have established a multifaceted role of *Nkx6.1* in the differentiation of neurons and glia during embryonic spinal cord development (Sander et al., 2000; Vallstedt et al., 2001; Zhao et al., 2014). Thus, the finding that *Nkx6.1* expression increases the number of cholinergic interneurons implies a similar neural differentiation function of *Nkx6.1* in the adult injured spinal cord. However, it is not clear whether the increased number of cholinergic interneurons were generated from NSPCs. Our future research will include lineage tracing experiments to confirm that *Nkx6.1* expression promotes the generation of new neurons. Although the molecular mechanisms underlying *Nkx6.1* function in the adult remain elusive, our results support a potential role for *Nkx6.1* in regulating NSPC activation and subsequent differentiation. Studies have shown that Notch1 expression in vivo was transiently enhanced in response to injury (Yamamoto et al., 2001). In addition, our previous studies have shown that *Nkx6.1* regulates Notch1 expression in the NSPCs of the developing spinal cord (Li et al., 2016). Consistent with the notion that Notch signaling involves in injury response, *Nkx6.1* expression further transiently upregulates Notch signaling and increases

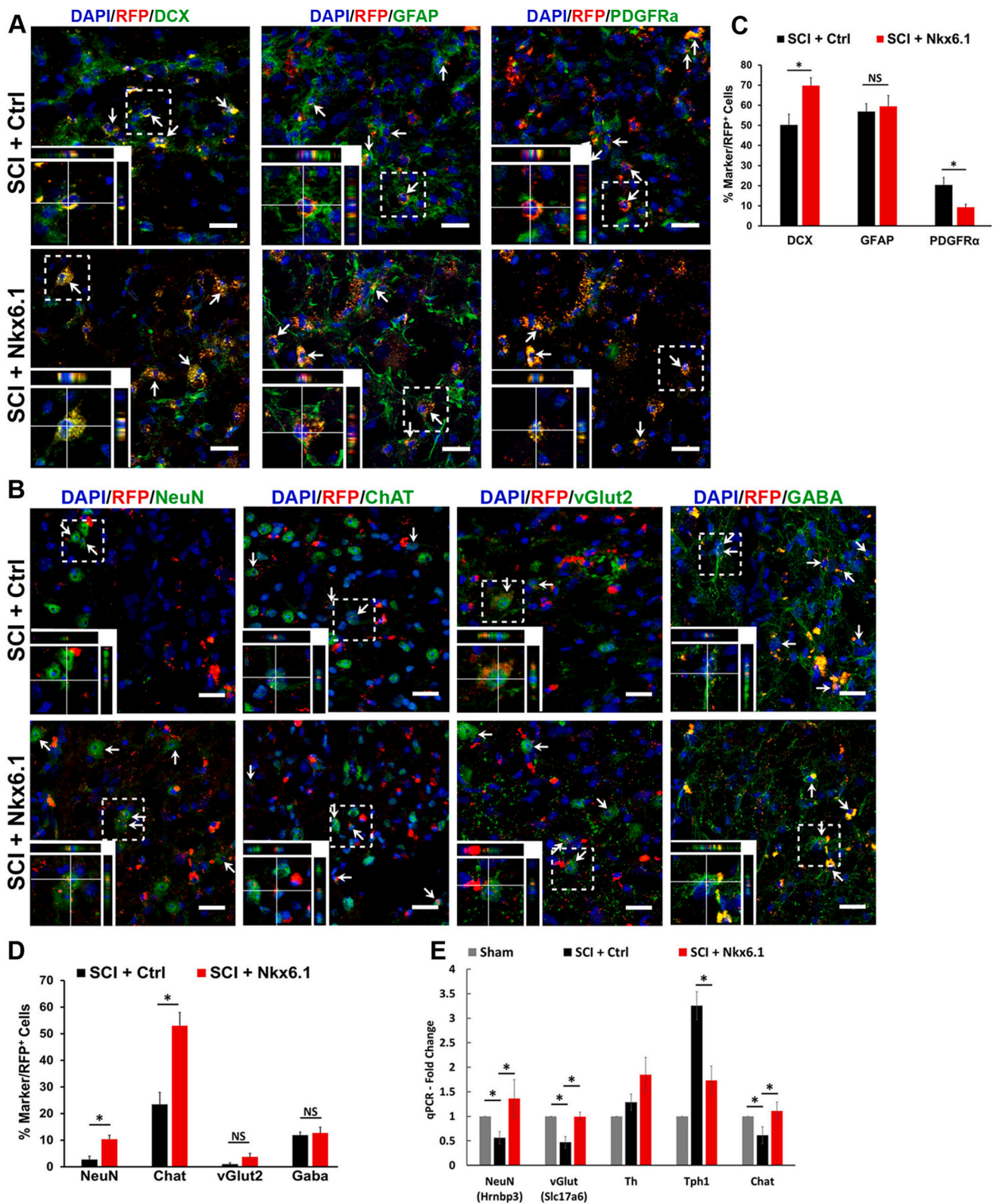


**Fig. 5.** Nkx6.1 increases the number of cholinergic interneurons in the injured spinal cord. Spinal cord tissues were harvested and analyzed for the effect of Nkx6.1 expression on cellular composition and gene expression. Representative confocal images of the sagittal section of spinal cord tissue samples stained for the expression of early neural markers: doublecortin (DCX), GFAP, and PDGFR $\alpha$  at 14 DPI (A) and mature neural markers: NeuN, ChAT, vGlut2, and GABA at 56 DPI (B). The bottom left shows a higher magnification of an orthogonal view of the area denoted by a white box. Arrows indicate the co-labeling of the virally transduced (RFP<sup>+</sup>) cells with cell specific markers. Nuclei were counterstained with DAPI. Scale bars = 20  $\mu$ m. (C and D) Quantification of virally transduced cells co-labeled with cell specific marker. n = 3. \*p-value < 0.05, Mean  $\pm$  SEM; Student's *t*-test. (E) The qPCR analysis of the mRNA level of genes associated with mature neurons and specific neuronal cell types at 35 DPI. n  $\geq$  3/group. Mean  $\pm$  SEM; \*p-value < 0.05; One-way ANOVA followed by Tukey post-hoc test.

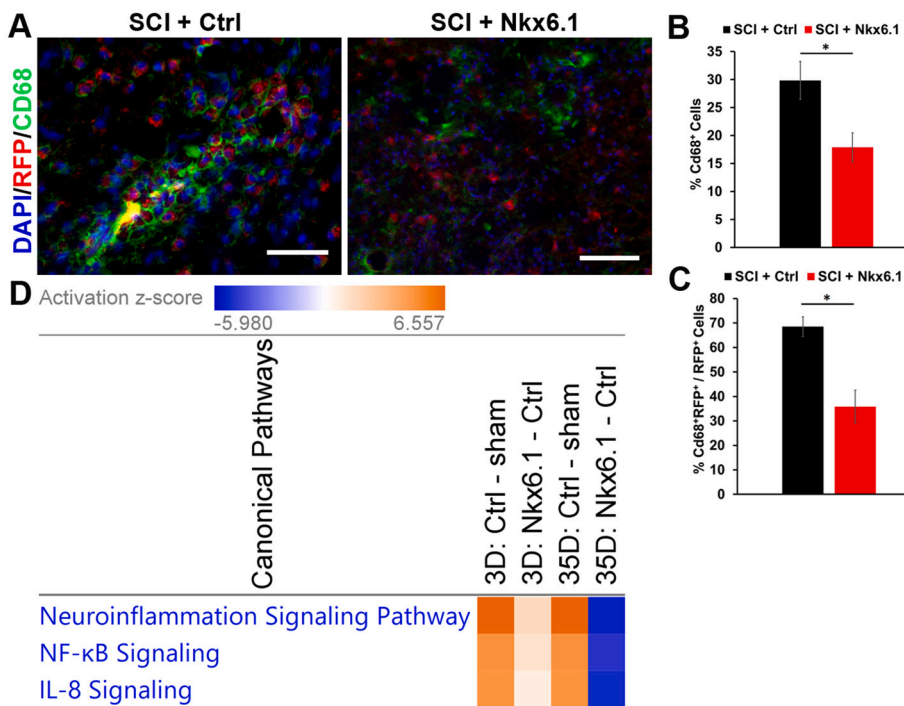


**Fig. 6.** Nkx6.1 expression attenuates neuroinflammation after SCI. Spinal cord tissues were harvested and analyzed for the effect of Nkx6.1 expression on neuroinflammation. (A) Representative image of the sagittal section of spinal cord tissue samples at 3 DPI and analyzed for macrophage marker CD68. Nuclei were counterstained with DAPI. Scale bars = 50  $\mu$ m. Quantification of percentage of CD68<sup>+</sup> cells among the total number of cells (B) and among RFP<sup>+</sup> cells (C) around injury/injection site. n = 3/group. Mean  $\pm$  SEM; \*p-value <0.05; Student's *t*-test. (D) Nkx6.1 expression significantly reduced pathway involved in neuroinflammation signaling, NF- $\kappa$ B signaling and IL-8 signaling by RNA-seq and ingenuity pathway analysis of differentially expressed genes.

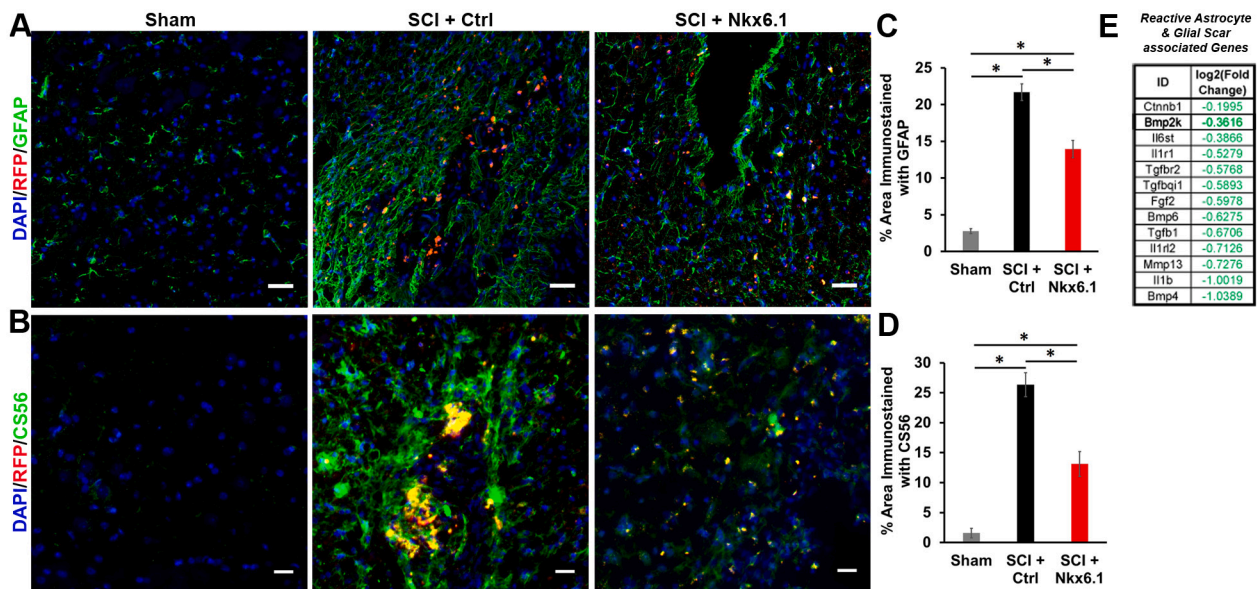


**Fig. 7.** Nkx6.1 attenuates the glial scar in the injured spinal cord. Spinal cord tissues were harvested and analyzed for the effect of Nkx6.1 expression on glial scar formation. Representative confocal images of the sagittal section of spinal cord tissue samples at 56 DPI and analyzed for reactive astrocyte marker GFAP (A) and chondroitin sulfate proteoglycan (CSPG) marker CS56 (B). Nuclei were counterstained with DAPI. Quantification of the area immunostained with anti-GFAP (C) and anti-CS56 antibodies (D). (E) A list of differentially expressed genes and their log2(fold change) by RNA-Seq analysis between the SCI + Ctrl group and SCI + Nkx6.1 group that are associated with reactive astrocyte (RA) and glial scar formation at 35 DPI. n  $\geq$  3. Mean  $\pm$  SEM; \*p-value < 0.05; One-way ANOVA followed by Tukey post-hoc test.

the number of Nestin<sup>+</sup> NSPCs in the acute phase of injury, suggesting a possible mechanism of Nkx6.1 in neural differentiation via Notch signaling.

Glial scar formation is a reactive cellular process involving astrogliosis that occurs after SCI (Faulkner et al., 2004). Reactive astrocytes are the main cellular components of the glial scar (Stichel and Müller, 1998). Previous studies have shown that ectopic expression of Nkx6.1 in native astrocytes (GFAP<sup>+</sup>) failed to induce their conversion into neurons (Matsui et al., 2014; Su et al., 2014), suggesting Nkx6.1 may not be a

potent factor for cell lineage reprogramming. Intriguingly, Nkx6.1 expression reduced glial scar formation, suggesting a possibility that Nkx6.1 promotes NSPC differentiation preferentially into neuron lineage at the expense of astroglial lineage. Thus, it is possible that the increased number of neurons is from Nkx6.1 induced NSPC differentiation. However, this needs to be confirmed by cell lineage tracing study or exclusive expression of Nkx6.1 in the NSPC population using NSPC-specific promoter. This is an important direction for our future research.

The activated microglia are an essential component of the

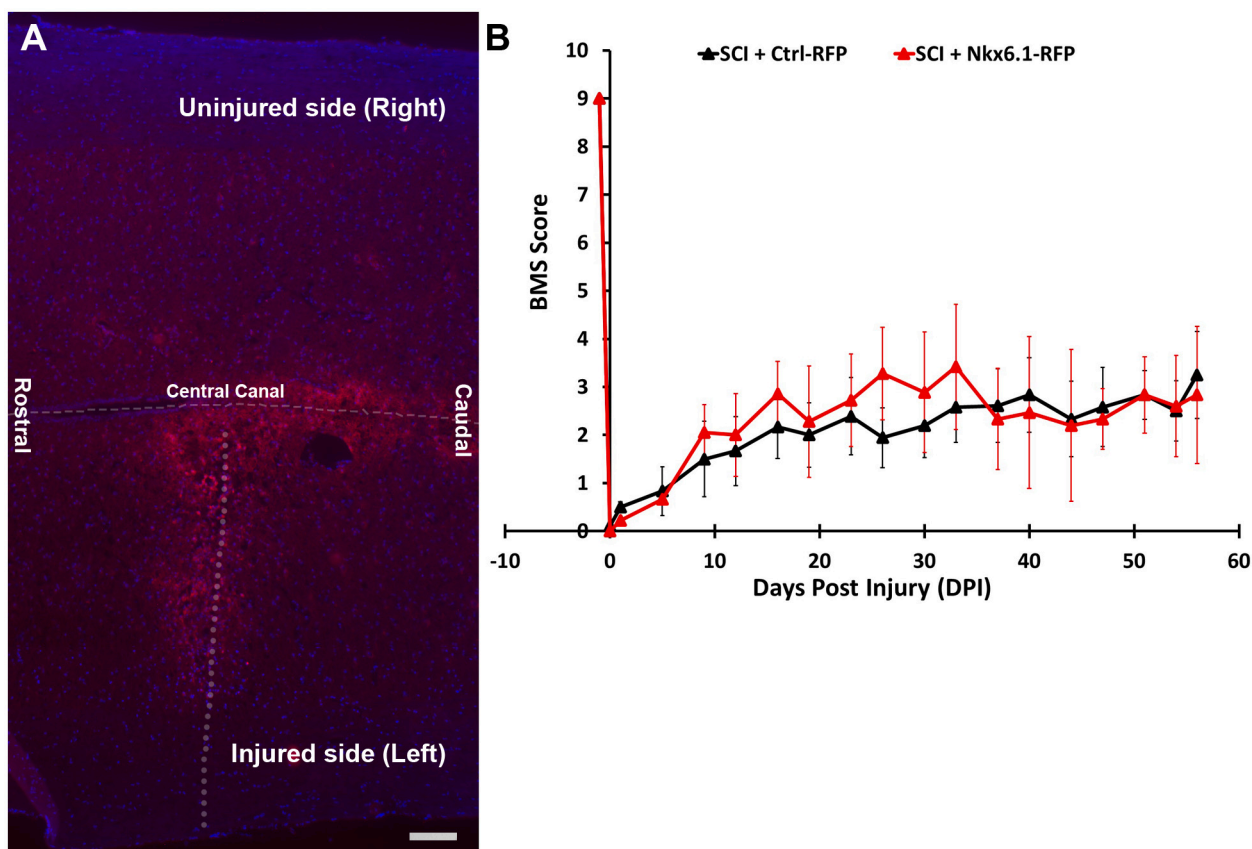


**Fig. 8.** Nkx6.1 expression did not improve locomotor function.

Lateral hemisection SCI was performed on 8–12 weeks old mice at the thoracic vertebrae (T10) level followed by lentivirus injection. (A) a representative image of the sagittal section around the injection site. Dashed line indicates the central canal and dotted line indicates the hemisection site. Red dots represent RFP+ cells. Cell nuclei were counter-stained with DAPI in blue. Scale bar = 100  $\mu$ m. Open field test was performed to assess locomotor functional recovery after Nkx6.1 expression. (B) A plot of the BMS scores of the left hindlimb from the day before injury to 56 DPI ( $n \geq 3$  for each timepoint and group). Two-way repeated measures ANOVA. No significant differences were observed at all time-points. (For interpretation of the references to colour in this figure legend, the reader is referred to the web version of this article.)

neuroprotective scar and represent an inflammatory process in response to SCI (Bellver-Landete et al., 2019). We found that Nkx6.1 significantly reduced the number of CD68<sup>+</sup> microglia as well as the expression of genes and pathways involved in neuroinflammation. The effect of Nkx6.1 on neuroinflammation has not been reported. Our results suggest a potential application of Nkx6.1 expression for anti-inflammation management in the treatment of SCI.

It is puzzling that even with an increased number of interneurons, reduced neuroinflammation, and minimized glial scar, there was no significant improvement in locomotor function. We speculate that in addition to the reduced glial scar and neuroinflammation, functional recovery may require the restoration of a damaged local neural circuit with proper types of functional neurons. It further indicates that the increase of cholinergic interneurons alone may not be sufficient to reconstruct the local neural circuit. A combination of different types of neurons may be required for this process. In support of this notion, we found that the forced expression of Gsx1 modulates the number of glutamatergic, cholinergic neurons, and GABAergic neurons as well as a reduced glial scar, which leads to a significant functional recovery (Patel et al., 2021).

In summary, we demonstrate that Nkx6.1 was able to reduce reactive astrocytes and glial scar and increase the number of cholinergic interneurons in the adult injured spinal cord. This study provides evidence that Nkx6.1 might be a potential gene for the manipulation of the glial scar, neuroinflammation, and the generation of interneurons in the adult injured spinal cord.

## 4. Materials and Methods

### 4.1. Lentivirus

pLenti-GIII-CMV-RFP-2A-Puro lentiviral vector with Nkx6.1-RFP (9947 bps) gene insert was purchased from Applied Biological Materials Inc. (Cat. # LV476460). The expression of Nkx6.1 and RFP is under the control of the promoter of CMV and SV40, respectively. The presence of a gene in the lentiviral vector was verified using PCR followed by gel electrophoresis. A lentiviral vector expressing only RFP was used as a negative control (lenti-Ctrl-RFP). Human Embryonic Kidney (HEK293T) cells were cultured in high glucose Dulbecco's Modified Eagle Media (DMEM) supplemented with 10% fetal bovine serum (FBS), 1% non-essential amino acid (NEAA), and 1% Glutamax. Once the HEK293T cells were about 50%–60% confluent, they were transfected with target vector (lenti-Nkx6.1-RFP or lenti-Ctrl-RFP), envelope plasmid (pMD2.G/VSVG, Addgene 12259), and 3rd generation packaging plasmids (pMDLg/pRRE, Addgene 12251 and pRSV-Rev, Addgene 12253). The virus-containing supernatant was collected at two- and four-days post-transfection. Once all supernatant was collected on day two, fresh media was added to the cells. Viral particles were concentrated by polyethylene glycol 6000 (PEG6000) method (Kutner et al., 2009) and titer was determined by infecting HEK293T cells (Kutner et al., 2009).

### 4.2. Lateral hemisection spinal cord injury (SCI) and lentivirus injection

All experimental protocols were approved by the Institutional

Animal Care and Use Committee (IACUC) and the Institutional Biosafety Committee at Rutgers University. All animal work was conducted in accordance with relevant guidelines and regulations of the IACUC. Young adult C57BL/6 mice (8–12 weeks-old) were used for this study. Mice (both males and females) were kept at a 12-h light/dark cycle and were blindly and randomly chosen for each treatment condition. Animals were divided into the following groups (3 animals/group): (1) the sham group (the skin and muscle were cut to expose the spine, but SCI was not performed), (2) mice received SCI and lenti-Ctrl-RFP treatment (SCI + Ctrl), and (3) mice received SCI and lenti-Nkx6.1-RFP treatment (SCI + Nkx6.1). For SCI groups, a lateral hemisection was performed by first exposing the spinal cord around T9-T10 by laminectomy and then laterally cut on the left side of the spinal cord from the midline to the end. Immediately after the SCI, two injections of 1.0  $\mu$ l of lentiviral particles ( $1 \times 10^7$  TU/ml) each at  $\sim$ 1 mm rostral and caudal to the lesion site, respectively. The needle was kept in place for 2–3 min after the injection to avoid backflow and allow virus diffusion into the tissue. The wound was then sealed by stitching the muscle and 2–3 clips on the skin. After surgery, animals from all three groups subcutaneously received painkiller (1 mg/kg Meloxicam) and antibiotics (50 mg/kg Cefazoline). Completeness of the hemisection was determined by the observation of paralysis in the left hind limb at the day-post injury (0 DPI) and 1 DPI.

#### 4.3. Behavioral/locomotor assessment

Locomotion behavior of each animal was evaluated based on the Basso Mouse Scale (BMS) from an open field test (Basso et al., 2006). BMS scale ranges from 0 (completely paralyzed) to 9 (normal). The BMS score assessment was given 4 min of observation per animal by three independent observers who are blinded to the type of treatment. The BMS assessment was performed once before the surgery and then twice a week until 56 DPI.

#### 4.4. Tissue processing

Spinal cord tissues were harvested at 3, 14, 35, and 56 DPI ( $n = 3$ /group/time point). At each time point, mice were intracardially perfused with  $1 \times$  (v/v) sterile phosphate buffer saline followed by 4% (w/v) paraformaldehyde (PFA). About 5–6 mm of the spinal cord tissue containing the injury and injection sites was removed and fixed overnight with 4% PFA. The next day, fixed tissue was washed with  $1 \times$  PBS and transferred to 30% (w/v) sucrose for dehydration for about 24 h. Dehydrated tissue was embedded using Tissue-Tek<sup>®</sup> optimum cutting temperature (O.C.T.) and stored at  $-80$  °C. At each time point, tissues were sectioned on the sagittal plane at 12  $\mu$ m thickness using a cryostat (ThermoScientific).

#### 4.5. Immunohistochemistry (IHC)

IHC was performed based on a previously established protocol with minor modifications (Li et al., 2016). The sections were treated with cold methanol for 10 mins at room temperature, followed by incubating samples with blocking solution (0.05% Triton X-100, 2% donkey serum, and 3% bovine serum albumin (BSA)) to reduce background signal. Then, samples were incubated with primary antibodies (Table S1) in  $1 \times$  (v/v) phosphate buffer saline (PBS) overnight at 4 °C. The next day, samples were washed with  $1 \times$  PBS and incubated with secondary antibodies (Table S1) for 1 h at room temperature. Lastly, samples were washed with  $1 \times$  PBS and incubated with DAPI (200 ng/ml) for 5 mins followed by the final wash and the slides were sealed with Cytoseal 60 (ThermoFisher Scientific 8310–4).

#### 4.6. Image analysis

For image analysis, at least five sections from each slide (each with different antibodies)/animal were analyzed. Images were captured at

the same exposure and threshold, and at the same intensity per condition using Zeiss LSM 800 confocal microscope or Zeiss AxioVision Imager A.1. The automatic cell counter in ImageJ (Rueden et al., 2017; Schneider et al., 2012) was used to count the total number of cells. Co-labeled cells with cell type-specific markers and viral marker RFP were counted manually in separate RGB channels and with the following stereological considerations: 1) systematic and random sampling; 2) calculation of total cell numbers instead of signal densities, 3) counting of cells with aid from DAPI staining, not cell profiles, and 4) specific staining to identify the cells of interest. Data were presented as the mean  $\pm$  standard error of the mean (SEM). Statistical significance between two conditions was calculated by Student's *t*-test and multi-group comparisons were performed using one-way ANOVA, followed by Tukey post-hoc test. A *p*-value of less than 0.05 was considered statistically significant.

#### 4.7. RNA isolation

For RNA isolation, about 5 mm small region of the spinal cord tissue (containing the injury and the injection site) were extracted at 3 and 35 DPI, to reduce the heterogeneity due to the treatment and no treatment. At least 3 samples for each condition per timepoint were harvested. Total RNA from spinal cord tissue was preserved by fast freezing the tissue samples in liquid nitrogen. Total RNA was isolated from spinal cord tissue using RNeasy Lipid Tissue Mini kit (Qiagen, #74804) using the manufacturer's protocol. Total RNA was treated with DNase I (Qiagen) to eliminate genomic DNA contamination. The concentration and the quality of the total RNA were determined by NanoDrop Lite Spectrophotometer (ThermoScientific).

#### 4.8. Real-time quantitative PCR (qPCR) analysis

From the total RNA, complementary DNA (cDNA) was synthesized using SuperScript III First-Strand Synthesis System (Invitrogen, #18080051) using the manufacturer's protocol. qPCR was performed with Power SYBR<sup>™</sup> Green PCR Master Mix and gene-specific primers (Table S2) using StepOnePlus Real-Time PCR system (Applied Biosystem). Glyceraldehyde 3-phosphate dehydrogenase (GAPDH) was used as a housekeeping gene. The Livak method was used to calculate the fold change of SCI + Ctrl and SCI + Nkx6.1 groups normalized to the sham group.

#### 4.9. Library preparation and RNA-seq analysis

Quality control of the total RNA (using RNA 6000 Nano chip on the 2100 Bioanalyzer), library preparation (Illumina MiSeq) and RNA-Seq were performed by Admera Health (South Plainfield, NJ). The RNA-Seq was performed at 3 DPI and 35 DPI ( $n = 3$ /group/time point) using Illumina MiSeq using the manufacturer's protocol. Each sample was sequenced as paired-end ( $2 \times 150$  bp) on the Illumina MiSeq platform and generated a total of 40 million reads per sample.

Quality of the raw fastq file was assessed using the FastQC (<http://www.bioinformatics.babraham.ac.uk/projects/fastqc/>). Once the sample passed quality control (QC) all sequences were aligned to the mouse reference genome, mm10, using STAR (version 2.0; Dobin et al., 2013). The raw read counts were assembled as a matrix using HTSeq (version 0.6.0; Anders et al., 2015) and normalized using the DESeq2 (Anders and Huber, 2010; Love et al., 2014), a R/Bioconductor package. Next, DESeq2 was used to call for differential expressed gene (DEGs;  $p < 0.05$ ) from the count matrix. The downstream pathway analysis was carried out using the Ingenuity Pathway Analysis (IPA, QIAGEN, Inc., <http://www.qiagenbioinformatics.com/products/ingenuity-pathway-analysis>; Kramer et al., 2014).

## Data availability

The raw RNA-seq gene expression data described in this manuscript have been deposited in NCBI's Gene Expression Omnibus and are accessible through the GEO series accession number GSE171441.

## Authors' contributions

**M.P.:** Methodology, Investigation, Visualization, Formal analysis, Writing – original draft. **J.A., S.L., Z.F., B.R., F.E., R.R., Y.L., K.B.L.:** Investigation, Visualization, Formal analysis. **Y.L.L.:** Conceptualization, Methodology, Formal analysis. **L.C.:** Conceptualization, Methodology, Visualization, Formal analysis, Writing – original draft, review and editing, Supervision, Project administration, Funding acquisition.

## Declaration of Competing Interests

The authors declare no competing interests.

## Acknowledgement

We thank members of the Cai lab for their constructive comments and discussion, Dr. Kelvin Kwan for advice on lentivirus production, and Dr. Ki-Bum Lee and members of his lab for advice on qPCR analysis. This work was supported by the State of New Jersey Commission on Spinal Cord Research 15IRG006 (L.C.), the U.S. Department of Education GAANN Precision and Personalized Medicine Pre-Doctoral Training Fellowship (M.P.), and the NIH Biotechnology Pre-Doctoral Training Fellowship T32GM008339 (M.P. and J.A.). K.B.L acknowledges partial financial support from the NSF (CHE-1429062) and NIH R01 (1R01DC016612).

## Appendix A. Supplementary data

Supplementary data to this article can be found online at <https://doi.org/10.1016/j.expneurol.2021.113826>.

## References

- Ables, J.L., Breunig, J.J., Eisch, A.J., Rakic, P., 2011. Not(ch) just development: notch signalling in the adult brain. *Nat. Rev. Neurosci.* 12, 269–283.
- Alexander, J.K., Popovich, P.G., 2009. Neuroinflammation in spinal cord injury: therapeutic targets for neuroprotection and regeneration. *Prog. Brain Res.* 175, 125–137.
- Anders, S., Huber, W., 2010. Differential expression analysis for sequence count data. *Genome Biol.* 11, R106.
- Anders, S., Pyl, P.T., Huber, W., 2015. HTSeq—a Python framework to work with high-throughput sequencing data. *Bioinformatics* 31, 166–169.
- Barnabe-Heider, F., Frisen, J., 2008. Stem cells for spinal cord repair. *Cell Stem Cell* 3, 16–24.
- Basso, D.M., Fisher, L.C., Anderson, A.J., Jakeman, L.B., McTigue, D.M., Popovich, P.G., 2006. Basso mouse scale for locomotion detects differences in recovery after spinal cord injury in five common mouse strains. *J. Neurotrauma* 23, 635–659.
- Bellver-Landete, V., Bretheau, F., Mailhot, B., Vallieres, N., Lessard, M., Janelle, M.E., Vernoux, N., Tremblay, M.E., Fuehrmann, T., Shoichet, M.S., Lacroix, S., 2019. Microglia are an essential component of the neuroprotective scar that forms after spinal cord injury. *Nat. Commun.* 10, 518.
- Benner, E.J., Luciano, D., Jo, R., Abdi, K., Paez-Gonzalez, P., Sheng, H., Warner, D.S., Liu, C., Eroglu, C., Kuo, C.T., 2013. Protective astrogenesis from the SVZ niche after injury is controlled by notch modulator Thbs4. *Nature* 497, 369–373.
- Briscoe, J., Sussell, L., Serup, P., Hartigan-O'Connor, D., Jessell, T.M., Rubenstein, J.L., Ericson, J., 1999. Homeobox gene Nkx2.2 and specification of neuronal identity by graded sonic hedgehog signalling. *Nature* 398, 622–627.
- Cai, J., Xu, X., Yin, H., Wu, R., Modderman, G., Chen, Y., Jensen, J., Hui, C.C., Qiu, M., 2000. Evidence for the differential regulation of Nkx-6.1 expression in the ventral spinal cord and foregut by Shh-dependent and -independent mechanisms. *Genesis* 27, 6–11.
- Chen, W., Zhang, B., Xu, S., Lin, R., Wang, W., 2017. Lentivirus carrying the NeuroD1 gene promotes the conversion from glial cells into neurons in a spinal cord injury model. *Brain Res. Bull.* 135, 143–148.
- Dobin, A., Davis, C.A., Schlesinger, F., Drenkow, J., Zaleski, C., Jha, S., Batut, P., Chaisson, M., Gingeras, T.R., 2013. STAR: ultrafast universal RNA-seq aligner. *Bioinformatics* 29, 15–21.
- Fabbiani, G., Rehermann, M.I., Aldecosea, C., Trujillo-Ceno, O., Russo, R.E., 2018. Emergence of serotonergic neurons after spinal cord injury in turtles. *Front. Neural Circuits* 12, 20.
- Faulkner, J.R., Herrmann, J.E., Woo, M.J., Tansey, K.E., Doan, N.B., Sofroniew, M.V., 2004. Reactive astrocytes protect tissue and preserve function after spinal cord injury. *J. Neurosci.* 24, 2143–2155.
- Fawcett, J.W., Asher, R.A., 1999. The glial scar and central nervous system repair. *Brain Res. Bull.* 49, 377–391.
- Fu, H., Qi, Y., Tan, M., Cai, J., Hu, X., Liu, Z., Jensen, J., Qiu, M., 2003. Molecular mapping of the origin of postnatal spinal cord ependymal cells: evidence that adult ependymal cells are derived from Nkx6.1+ ventral neural progenitor cells. *J. Comp. Neurol.* 456, 237–244.
- Gensel, J.C., Zhang, B., 2015. Macrophage activation and its role in repair and pathology after spinal cord injury. *Brain Res.* 1619, 1–11.
- Givogri, M.I., de Planell, M., Galbati, F., Superchi, D., Gritti, A., Vescovi, A., de Vellis, J., Bongarzone, E.R., 2006. Notch signaling in astrocytes and neuroblasts of the adult subventricular zone in health and after cortical injury. *Dev. Neurosci.* 28, 81–91.
- Hackett, A.R., Lee, J.K., 2016. Understanding the NG2 glial scar after spinal cord injury. *Front. Neurol.* 7, 199.
- Hackett, A.R., Lee, D.H., Dawood, A., Rodriguez, M., Funk, L., Tsoulfas, P., Lee, J.K., 2016. STAT3 and SOCS3 regulate NG2 cell proliferation and differentiation after contusive spinal cord injury. *Neurobiol. Dis.* 89, 10–22.
- Hara, M., Kobayakawa, K., Ohkawa, Y., Kumamaru, H., Yokota, K., Saito, T., Kijima, K., Yoshizaki, S., Harimaya, K., Nakashima, Y., Okada, S., 2017. Interaction of reactive astrocytes with type I collagen induces astrocytic scar formation through the integrin-N-cadherin pathway after spinal cord injury. *Nat. Med.* 23, 818–828.
- Jones, L.L., Margolis, R.U., Tuszynski, M.H., 2003. The chondroitin sulfate proteoglycans neurocan, brevican, phosphacan, and versican are differentially regulated following spinal cord injury. *Exp. Neurol.* 182, 399–411.
- Kirdajova, D., Anderova, M., 2020. NG2 cells and their neurogenic potential. *Curr. Opin. Pharmacol.* 50, 53–60.
- Kramer, A., Green, J., Pollard Jr., J., Tugendreich, S., 2014. Causal analysis approaches in ingenuity pathway analysis. *Bioinformatics* 30, 523–530.
- Kuscha, V., Frazer, S.L., Dias, T.B., Hibi, M., Becker, T., Becker, C.G., 2012. Lesion-induced generation of interneuron cell types in specific dorsoventral domains in the spinal cord of adult zebrafish. *J. Comp. Neurol.* 520, 3604–3616.
- Kutner, R.H., Zhang, X.Y., Reiser, J., 2009. Production, concentration and titration of pseudotyped HIV-1-based lentiviral vectors. *Nat. Protoc.* 4, 495–505.
- LeComte, M.D., Shimada, I.S., Sherwin, C., Spees, J.L., 2015. Notch1-STAT3-ETBR signaling axis controls reactive astrocyte proliferation after brain injury. *Proc. Natl. Acad. Sci. U. S. A.* 112, 8726–8731.
- Li, Y., Tzatzalos, E., Kwan, K.Y., Grumet, M., Cai, L., 2016. Transcriptional regulation of Notch1 expression by Nkx6.1 in neural stem/progenitor cells during ventral spinal cord development. *Sci. Rep.* 6, 38665.
- Love, M.I., Huber, W., Anders, S., 2014. Moderated estimation of fold change and dispersion for RNA-seq data with DESeq2. *Genome Biol.* 15, 550.
- Matsui, T., Akamatsu, W., Nakamura, M., Okano, H., 2014. Regeneration of the damaged central nervous system through reprogramming technology: basic concepts and potential application for cell replacement therapy. *Exp. Neurol.* 260, 12–18.
- McKay, S.M., Brooks, D.J., Hu, P., McLachlan, E.M., 2007. Distinct types of microglial activation in white and grey matter of rat lumbosacral cord after mid-thoracic spinal transection. *J. Neuropathol. Exp. Neurol.* 66, 698–710.
- McKeon, R.J., Hoke, A., Silver, J., 1995. Injury-induced proteoglycans inhibit the potential for laminin-mediated axon growth on astrocytic scars. *Exp. Neurol.* 136, 32–43.
- McKeon, R.J., Juryne, M.J., Buck, C.R., 1999. The chondroitin sulfate proteoglycans neurocan and phosphacan are expressed by reactive astrocytes in the chronic CNS glial scar. *J. Neurosci.* 19, 10778–10788.
- Meletis, K., Barnabe-Heider, F., Carlen, M., Evergren, E., Tomilin, N., Shupliakov, O., Frisen, J., 2008. Spinal cord injury reveals multilineage differentiation of ependymal cells. *PLoS Biol.* 6, e182.
- Milich, L.M., Ryan, C.B., Lee, J.K., 2019. The origin, fate, and contribution of macrophages to spinal cord injury pathology. *Acta Neuropathol.* 137, 785–797.
- Mothe, A.J., Tator, C.H., 2005. Proliferation, migration, and differentiation of endogenous ependymal region stem/progenitor cells following minimal spinal cord injury in the adult rat. *Neuroscience* 131, 177–187.
- Nishiyama, A., Komitova, M., Suzuki, R., Zhu, X., 2009. Polydendrocytes (NG2 cells): multifunctional cells with lineage plasticity. *Nat. Rev. Neurosci.* 10, 9–22.
- O'Shea, T.M., Burda, J.E., Sofroniew, M.V., 2017. Cell biology of spinal cord injury and repair. *J. Clin. Invest.* 127, 3259–3270.
- Patel, M., Li, Y., Anderson, J., Castro-Pedrido, S., Skinner, R., Lei, S., Finkel, Z., Rodriguez, B., Esteban, F., Lee, K., Lyu, Y., Cai, L., 2021. Gsx1 promotes locomotor functional recovery after spinal cord injury. *Mol. Ther.* 29 (8), 2469–2482. <https://doi.org/10.1016/j.ymthe.2021.04.027>. Epub 2021 Apr 23. PMID: 33895323.
- Pierfelice, T., Alberi, L., Gaiano, N., 2011. Notch in the vertebrate nervous system: an old dog with new tricks. *Neuron* 69, 840–855.
- Rhodes, K.E., Fawcett, J.W., 2004. Chondroitin sulphate proteoglycans: preventing plasticity or protecting the CNS? *J. Anat.* 204, 33–48.
- Rueden, C.T., Schindelin, J., Hiner, M.C., DeZonia, B.E., Walter, A.E., Arena, E.T., Elieci, K.W., 2017. ImageJ2: ImageJ for the next generation of scientific image data. *BMC Bioinformatics* 18, 529.
- Sabelstrom, H., Stenudd, M., Frisen, J., 2014. Neural stem cells in the adult spinal cord. *Exp. Neurol.* 260, 44–49.
- Sander, M., Paydar, S., Ericson, J., Briscoe, J., Berber, E., German, M., Jessell, T.M., Rubenstein, J.L., 2000. Ventral neural patterning by Nkx homeobox genes: Nkx6.1

- controls somatic motor neuron and ventral interneuron fates. *Genes Dev.* 14, 2134–2139.
- Schneider, C.A., Rasband, W.S., Eliceiri, K.W., 2012. NIH image to ImageJ: 25 years of image analysis. *Nat. Methods* 9, 671–675.
- Siddiqui, A.M., Khazaei, M., Fehlings, M.G., 2015. Translating mechanisms of neuroprotection, regeneration, and repair to treatment of spinal cord injury. *Prog. Brain Res.* 218, 15–54.
- Soderblom, C., Luo, X., Blumenthal, E., Bray, E., Lyapichev, K., Ramos, J., Krishnan, V., Lai-Hsu, C., Park, K.K., Tsoulfas, P., Lee, J.K., 2013. Perivascular fibroblasts form the fibrotic scar after contusive spinal cord injury. *J. Neurosci.* 33, 13882–13887.
- Stichel, C.C., Muller, H.W., 1998. The CNS lesion scar: new vistas on an old regeneration barrier. *Cell Tissue Res.* 294, 1–9.
- Su, Z., Niu, W., Liu, M.L., Zou, Y., Zhang, C.L., 2014. In vivo conversion of astrocytes to neurons in the injured adult spinal cord. *Nat. Commun.* 5, 3338.
- Tai, W., Wu, W., Wang, L.L., Ni, H., Chen, C., Yang, J., Zang, T., Zou, Y., Xu, X.M., Zhang, C.L., 2021. In vivo reprogramming of NG2 glia enables adult neurogenesis and functional recovery following spinal cord injury. *Cell Stem Cell* 28 (5), 923–937. <https://doi.org/10.1016/j.stem.2021.02.009>. Epub 2021 Mar 5. PMID: 33675690; PMCID: PMC8106641.
- Tessem, J.S., Moss, L.G., Chao, L.C., Arlotto, M., Lu, D., Jensen, M.V., Stephens, S.B., Tontonoz, P., Hohmeier, H.E., Newgard, C.B., 2014. Nkx6.1 regulates islet beta-cell proliferation via Nr4a1 and Nr4a3 nuclear receptors. *Proc. Natl. Acad. Sci. U. S. A.* 111, 5242–5247.
- Tran, A.P., Warren, P.M., Silver, J., 2018. The biology of regeneration failure and success after spinal cord injury. *Physiol. Rev.* 98, 881–917.
- Tzatzalos, E., Smith, S.M., Doh, S.T., Hao, H., Li, Y., Wu, A., Grumet, M., Cai, L., 2012. A cis-element in the Notch1 locus is involved in the regulation of gene expression in interneuron progenitors. *Dev. Biol.* 372, 217–228.
- Vallstedt, A., Muhr, J., Pattyn, A., Pierani, A., Mendelsohn, M., Sander, M., Jessell, T.M., Ericson, J., 2001. Different levels of repressor activity assign redundant and specific roles to Nkx6 genes in motor neuron and interneuron specification. *Neuron* 31, 743–755.
- Wang, H., Song, G., Chuang, H., Chiu, C., Abdelmaksoud, A., Ye, Y., Zhao, L., 2018. Portrait of glial scar in neurological diseases. *Int. J. Immunopathol. Pharmacol.* 31, 2058738418801406.
- Windle, W.F., Chambers, W.W., 1950. Regeneration in the spinal cord of the cat and dog. *J. Comp. Neurol.* 93, 241–257.
- Yamamoto, S., Nagao, M., Sugimori, M., Kosako, H., Nakatomi, H., Yamamoto, N., Takebayashi, H., Nabeshima, Y., Kitamura, T., Weinmaster, G., Nakamura, K., Nakafuku, M., 2001. Transcription factor expression and notch-dependent regulation of neural progenitors in the adult rat spinal cord. *J. Neurosci.* 21, 9814–9823.
- Zhao, X., Chen, Y., Zhu, Q., Huang, H., Teng, P., Zheng, K., Hu, X., Xie, B., Zhang, Z., Sander, M., Qiu, M., 2014. Control of astrocyte progenitor specification, migration and maturation by Nkx6.1 homeodomain transcription factor. *PLoS One* 9, e109171.